A Panchromatic, Near Infrared Ir(III) Emitter Bearing a Tripodal C^N^C ligand as a Dye for Dye-Sensitized Solar Cells

Claus Hierlinger,[a,b] Heather V. Flint,[c] David B. Cordes,[b] Alexandra M. Z. Slawin,[b] Elizabeth A. Gibson[c] Denis Jacquemin,*[d] Véronique Guerchais,*[a] Eli Zysman-Colman*[b]*

[a] Institut des Sciences Chimiques de Rennes, UMR 6226 CNRS-Université de Rennes 1, Campus de Beaulieu, 35042 Rennes Cedex, France. E-mail: veronique.guerchais@univ-rennes1.fr

[b] Organic Semiconductor Centre, EaStCHEM School of Chemistry, University of St Andrews, St Andrews, Fife, KY16 9ST, UK. E-mail: eli.zysman-colman@st-andrews.ac.uk; Web: http://www.zysman-colman.com

[c] Chemistry, School of Natural and Environmental Science, Newcastle University, Newcastle upon Tyne, NE1 7RU, UK. Elizabeth.gibson@ncl.ac.uk

[d] UMR CNRS 6230, Université de Nantes, CEISAM, 2 rue de la Houssinière, 44322 Nantes Cedex 3, France. E-mail: Denis.Jacquemin@univ-nantes.fr

Abstract

The synthesis of a new complex of the form [Ir(C^N^C)(N^N)Cl] [where C^N^C = 2-(bis(4-(*tert*-butyl)phenyl)methyl)pyridinato (d*t*Bubnpy, **L1**) and N^N is diethyl [2,2'-bipyridine]-4,4'-dicarboxylate (deeb)] is reported. The crystal structure reveals an unusual tripodal tridentate C^N^C ligand forming three six-membered rings around the iridium center. The photophysical and electrochemical properties suggest the use of this complex as a dye in dye-sensitized solar

cells. Time-Dependent Density Functional Theory (TD-DFT) calculations have been used to reveal the nature of the excited-states.

Introduction

Dye-sensitized solar cells (DSSCs) represent a promising solar cell technology. The majority of champion DSSCs, those showing power conversion efficiencies (PCE) greater than 10%, are based on ruthenium(II) complexes. Iridium(III) complexes, dominant as emitters in electroluminescent devices,[1,2] have to date fared poorly as dyes in DSSCs.[3-13] This is mainly because most iridium(III) complexes are not panchromatic, having absorption spectra that tail off by 550 nm. This induces low short circuit currents in the DSSC and as a consequence poor PCE; typically less than 4%. Indeed, there are very few examples of iridium(III) complexes with significant absorption bands going up to the red or NIR parts of the visible spectrum.[14-20,12]

We recently reported the development of tripodal C^N^C ligands, 2-benzhydrylpyridine and its derivatives, which can coordinate to iridium, forming three six-membered chelate rings through a double C-H bond activation.[21] When combined with a bidentate diimine ligand such as 4,4'-di*tert*butyl-2,2'-bipyridine (d*t*Bubpy), a family of orange-to-red emitting neutral [Ir(C^N^C)(d*t*Bubpy)Cl] complexes was formed with absorption bands tailing off at 600 nm. Herein, we report an analogous complex showing panchromatic absorption, employing an electron-poor ancillary ligand diethyl [2,2'-bipyridine]-4,4'-dicarboxylate (deeb), and study its use as a DSSC dye.

Results and Discussion

Synthesis

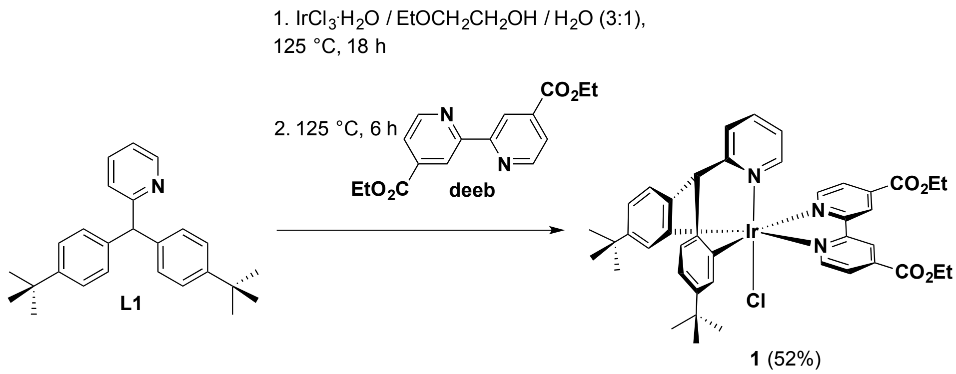

Scheme **1**: Scheme for the one-pot synthesis of complex **1**.

Compound **L1**[21] and deeb[22] were prepared by literature methods. Complex **1** was obtained as a black solid in 52% yield using a two-step-one-pot protocol wherein a mixture of **L1** and $IrCl_3.n6H_2O$ in 2-ethoxyethanol/H_2O (3:1) was heated at reflux for 19 h followed by the addition of deeb and a further reaction time of 6 h (Scheme **1**). Complex **1** was characterized by ^1H and ^{13}C NMR spectroscopy, HR-ESI mass spectrometry, elemental analysis and melting point determination [see Figures **S1-6** in the Supporting Information (SI) for NMR and HR-ESI mass spectra].

Crystal Structures

Single crystals of sufficient quality of **1** were grown from CH_2Cl_2/Et_2O at -18°C, and the structure of **1** was determined by single-crystal X-ray diffraction (Figure **1,** Table **S1**). Complex **1**, [Ir(**L1**)(deeb)Cl], lies in a mirror plane; the pyridyl ring of **L1**, the iridium(III) and the chloride all lying directly in the plane. The tridentate **L1** shows a tripodal chelation motif, analogous to that seen previously.[21] The remaining coordination sphere of **1** consists of the deeb N^N ligand and a chloride anion. The arrangement of ligands is unusual, as the chloride coordinates *trans* to the pyridine of **L1** and not *trans* to a cyclometalated carbon ligand as generally observed in tridentate complexes,[23-27] although this coordination arrangement was found in our previous complexes based on **L1**.[21] The Ir1-Cl1 bond is 2.346(3) Å, which is within the range of distances we have previously reported for [Ir(C^N^C)(d*t*Bubpy)Cl] complexes (where C^N^C is a substituted 2-benzhydrylpyridine),[21] and is similar to the Ir-Cl distance seen in the related complex $[Ir(tpy)(dmbpy)Cl]^{2+}$ (where tpy = 2,2':6',2"-terpyridine and dmbpy = 4,4'-dimethyl-2,2'-bipyridine).[28] The Ir-N_{N^N} bonds [Ir1-N18: 2.134(6) Å] are in the same range as both our related [Ir(C^N^C)(d*t*Bubpy)Cl] complexes,[21] as well as the deeb complex $[Ir(topy)_2(deeb)]PF_6$ [where topyH = 2-(*p*-tolyl)pyridine].[29] The Ir-N distance involving the nitrogen from **L1** [Ir1-N1: 2.038(8) Å] is markedly shorter than the Ir-N_{N^N} distance. The Ir-$C_{C^N^C}$ bonds [Ir1-C9: 2.027(7) Å] are shorter again than the Ir-N bonds, in agreement with our previous observations.[21] The bite angle of the N^N ligand is 76.1(3)°, in line with other iridium complexes possessing bidentate diimine ancillary ligands.[30-33,21] The C-Ir-C angle [85.2(4)°] and N-Ir-C angle within **L1** [88.0(2)°] are significantly larger due to the formation of three 6 membered chelate rings in the C^N^C ligand.

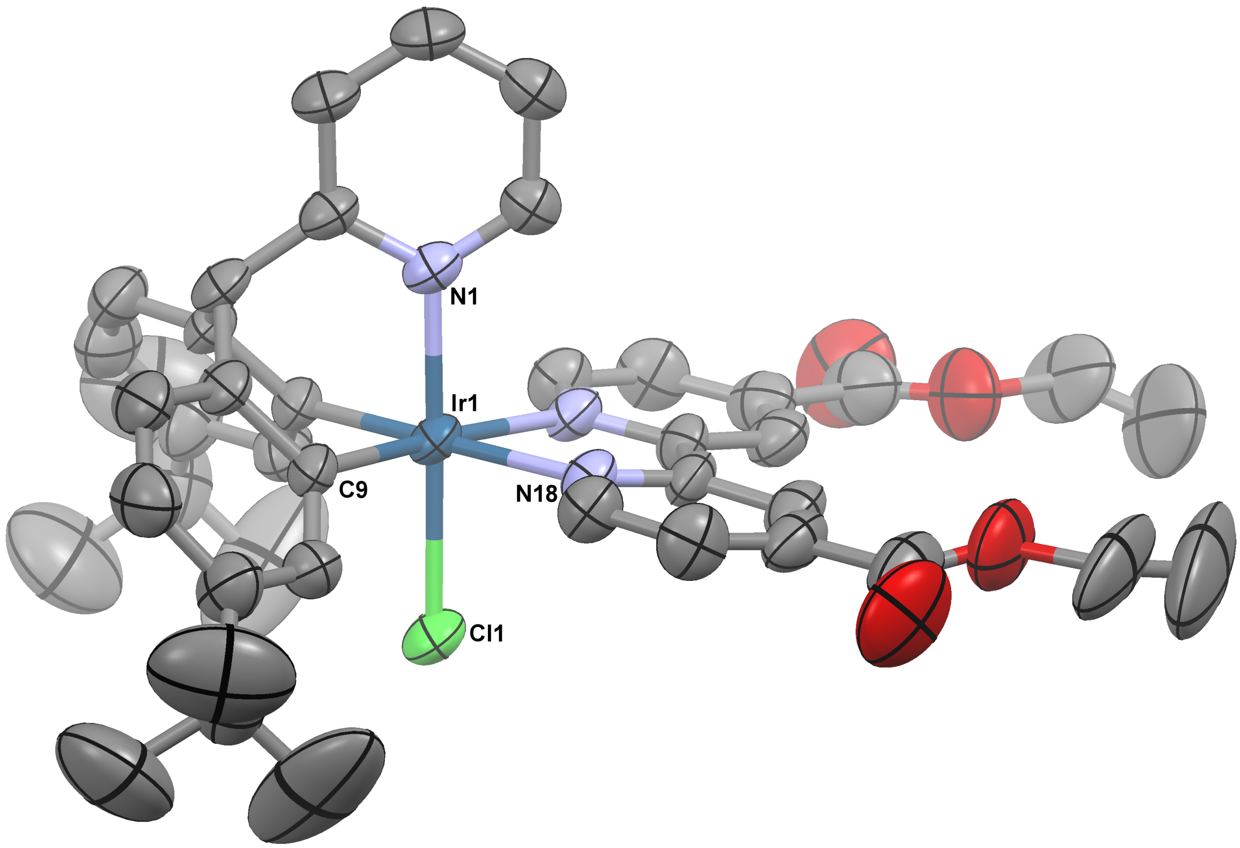

Figure **1**. Solid-state structure of complex **1**, thermal ellipsoids are drawn at the 50 % probability level. Hydrogen atoms and solvent molecules are omitted for clarity (color code: C = grey, N = purple, O = red, Cl = green and Ir = blue).

Electrochemical properties

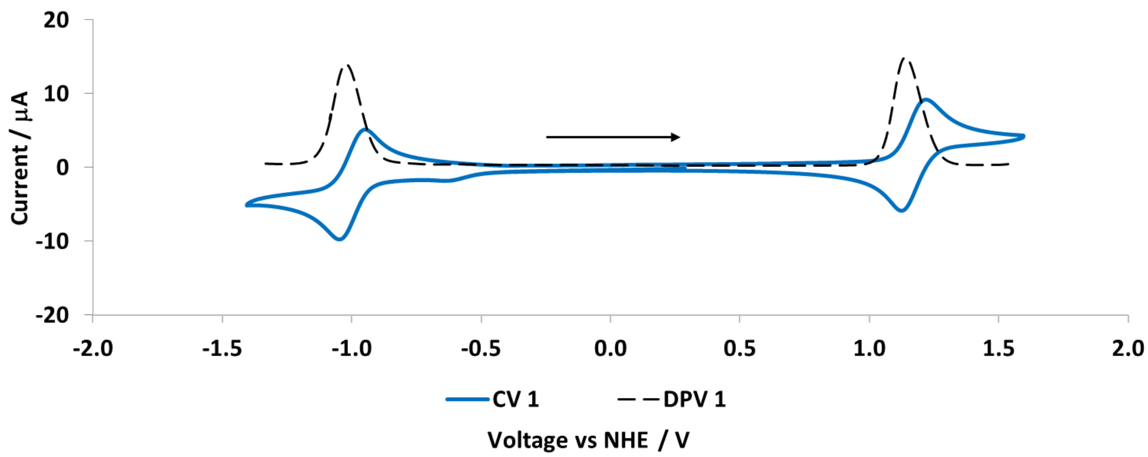

Figure **2**. Cyclic voltammograms (in blue solid lines) and differential pulse voltammetry (in dotted black lines) carried out in degassed CH_2Cl_2 at a scan rate of 100 mV s^{-1}, with Fc/Fc^+ as the internal reference, referenced to NHE (0.70 V vs. NHE).[34]

The electrochemical properties of **1** were evaluated by cyclic voltammetry (CV) and differential pulse voltammetry (DPV) in deaerated CH_2Cl_2 solution at 298 K at a scan rate of 100 mV s^{-1} using Fc/Fc^+ as the internal reference and referenced with respect to NHE (0.70 V vs. NHE).[34] The electrochemical data are summarized in Table **1** and the voltammograms are shown in Figure **2**. Complex **1** exhibits a quasi-reversible single electron oxidation wave at 1.21 V (ΔE_p = 88 mV), which is assigned to the Ir(III)/Ir(IV) redox couple, with contributions from the two phenyl rings of **L1** and the chloro ligand. Compared to [Ir(**L1**)(d*t*Bubpy)Cl], **R1**, (Figure **3**, $E_{1/2}^{ox.}$ 1.04 V vs. NHE)[21] the oxidation potential in **1** is significantly anodically shifted by 170 mV, reflecting the electron-withdrawing capacity of the ethyl ester groups of the N^N ligand, which modifies the electron density on iridium. However, the oxidation potential of **1** is less positive than that of [Ir(ppy)$_2$(deeb)]PF_6, **R2**, ($E_{1/2}^{ox.}$ = 1.57 V in deaerated MeCN vs NHE, where ppy is 2-phenylpyridinato).[35] Upon scanning to negative potential, **1** shows a single quasi-reversible reduction wave at -0.94 V (ΔE_p = 99 mV), which is monoelectronic as inferred from the DPV. The electron-withdrawing effect of the ethyl ester groups of the N^N ligand results in a large anodic shift of 610 mV in the reduction wave of **1** compared to **R1** ($E_{1/2}^{red.}$ -1.58 V vs NHE).[21] Complex **R2** showed two reversible reduction waves in MeCN. The first reduction located at -0.76 V is assigned to the reduction of the deeb ligand while the second one at -1.30 V is due to the reduction of the phenylpyridinato.[35] Thus, the reduction of the deeb ligand in **1** is shifted to more negative potentials compared to the same reduction in **R2**. DFT calculations of the previously reported **R1** indicated that both the HOMO and HOMO-1 are close in energy and involve the iridium and chlorine atoms and the two phenyl rings of **L1**.[21] As can be seen in Figure **4** the same electron density distribution is found in **1**. DFT calculations also show that the three lowest unoccupied orbitals are exclusively localized on the deeb ligand in **1** (Figure **4**), while the LUMO+1 is primarily on the pyridyl of **L1** in **R1**, illustrating the stronger accepting character of deeb. The $\Delta E_{\mathrm{redox}}$ for **1** (2.18 eV) is markedly smaller than that of **R2** ($\Delta E_{\mathrm{redox}}$ = 2.33 V).[35]

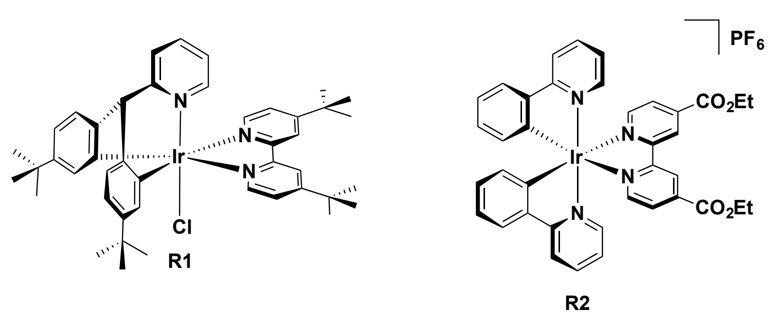

Figure **3**. Structures of reference complexes **R1** and **R2**.

Table **1**: Selected electrochemical properties of complex **1**

Electrochemistry[a]

	$E_{1/2}^{ox}$ / V	ΔE_p / mV	$E_{1/2}^{red}$ / V	ΔE_p / mV	ΔE_{redox}[b] / V	E_{HOMO}[c] /eV	E_{LUMO}[c] / eV
1	1.21	88	-0.97	99	2.18	-5.31	-3.13

[a] in degassed CH_2Cl_2 at a scan rate of 100 mV s^{-1} with Fc/Fc^+ as internal reference, and referenced with respect to NHE (Fc/Fc^+ = 0.70 V in CH_2Cl_2); [36,34,37] [36,34,37] [36,34,37] [b]ΔE_{redox} is the difference (V) between first oxidation and first reduction potentials; [c] $E_{HOMO/LUMO}$ = -[$E^{ox/red}$ vs Fc/Fc^+ + 4.8] eV.[34]

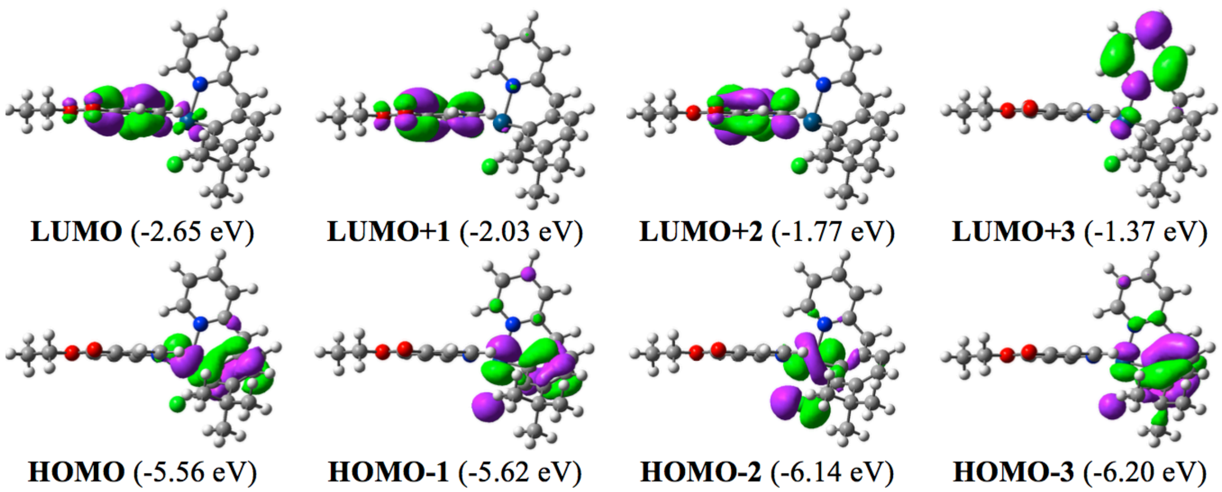

Figure **4**. Frontier molecular orbitals of **1** computed through DFT (M06 functional, see the SI for details) and represented using a contour threshold of 0.03 au.

Photophysical properties

The photophysical data for **1** recorded in CH_2Cl_2 at 298 K are shown in Figure **5** and the data summarized in Table **2**. The absorption profile of **1** differs significantly from that of **R1**. Complex **1** shows intense high-energy absorption bands (ε on the order of 3.5 × 10^4 M^{-1} cm^{-1}) below 250 nm, which are ascribed to $^1\pi$–π^* ligand-centered (^{1}LC) transitions localized on the deeb ligand. A moderately intense band (ε on the order of 1.5 × 10^4 M^{-1} cm^{-1}) at 319 nm is assigned to a ligand-centered (LC) transition on the deeb with a small CT character (see below). Weaker bands (ε on the order of 5-6 × 10^3 and 2 × 10^3 M^{-1} cm^{-1}) in the region of 380 – 440 nm and tailing to 500 - 600 nm are attributed to a mixture of (^{1}MLCT/^{1}LLCT) and spin-forbidden (^{3}MLCT/^{3}LLCT) transitions involving the deeb ligand. Iridium(III) complexes often do not show absorption onsets lower in energy than 550 nm;[38-40] though, there are known examples of neutral Ir(III) complexes showing absorption bands beyond 550 nm.[41,25,42,43]

The assignments for complex **1** were confirmed by TD-DFT calculations (see the ESI for technical details). The two lowest singlet states, computed at 623 and 611 nm, present relatively small intensities (oscillator strengths, *f*, of 0.010 and 0.056, respectively) and mainly correspond to HOMO-1 to LUMO and HOMO to LUMO transitions. As can be seen in Figure **4**, this clearly corresponds to a mixed CT process from the metal and the phenyl rings of the C^N^C ligand towards the deeb. The following significant vertical absorption are predicted by TD-DFT at 496 nm (f=0.071), 456 nm (f=0.027) and 443 nm (f=0.084) and these bands can be ascribed to HOMO-2 to LUMO, HOMO to LUMO+1 and HOMO-1 to LUMO+1 transitions, respectively, and therefore all involve strong CT character towards the deeb moiety. The more intense and resolved band at 319 nm experimentally (see Table **2**) is computed at 315 nm by TD-DFT (f=0.162) and corresponds to a more LC excitation from a low-lying orbital centered on the deeb (and partly on chlorine atom) towards the LUMO centered on the deeb as well.

Upon photoexcitation at 420 nm, **1** exhibits a broad featureless profile, indicative of an emission with mixed CT character, with a maximum at λ_{em} = 731 nm, an emission that is significantly redshifted (99 nm, 2194 cm^{-1}) compared to **R1** (λ_{em} = 630 nm).[21] The red-shifted luminescence is due to the presence of the presence of the π-accepting deeb. The emission of **1** is likewise red-shifted (51 nm, 2194 cm^{-1}) compared to that of **R2** (λ_{em} = 680 nm).[35] The DFT calculations returns an emission of the T_1 state at 762 nm, close to the experimental value, confirming emission from the lowest triplet excited state. The topology of this state, in terms of localization of the excess α electrons, is displayed in Figure **6**. As can be seen, the spin density is mostly localized on the Ir and Cl atoms and on the ancillary ligand, the tridentate ligand playing only a minor role in this state. This localization is consistent with the observed red-shift in emission compared to **R1** and **R2**. The measured photoluminescence quantum yield (Φ_{PL}) of **1** is 0.5%, lower than those of **R1** (6%) and **R2** (5%). This finding is a logical consequence of the energy gap law, which states that the nonradiative decay rate increases with decreasing emission energy.[44,45] Among near-infrared emissive cationic Ir(III) emitters with λ_{em} beyond 700 nm bearing diimines as ancillary ligand, most examples exhibit Φ_{PL} values less than 4%.[40,46-49] However, NIR-emitting neutral Ir(III) complexes of the form [Ir(C^N)$_2$(O^O)] (where O^O a substituted β-diketonate ancillary ligand) employing highly conjugated C^N ligands have reached Φ_{PL} of up to 16%.[50,41,51] Complex **1** exhibits a multiexponential emission decay, a reflection of the large non-radiative decay rate constant.

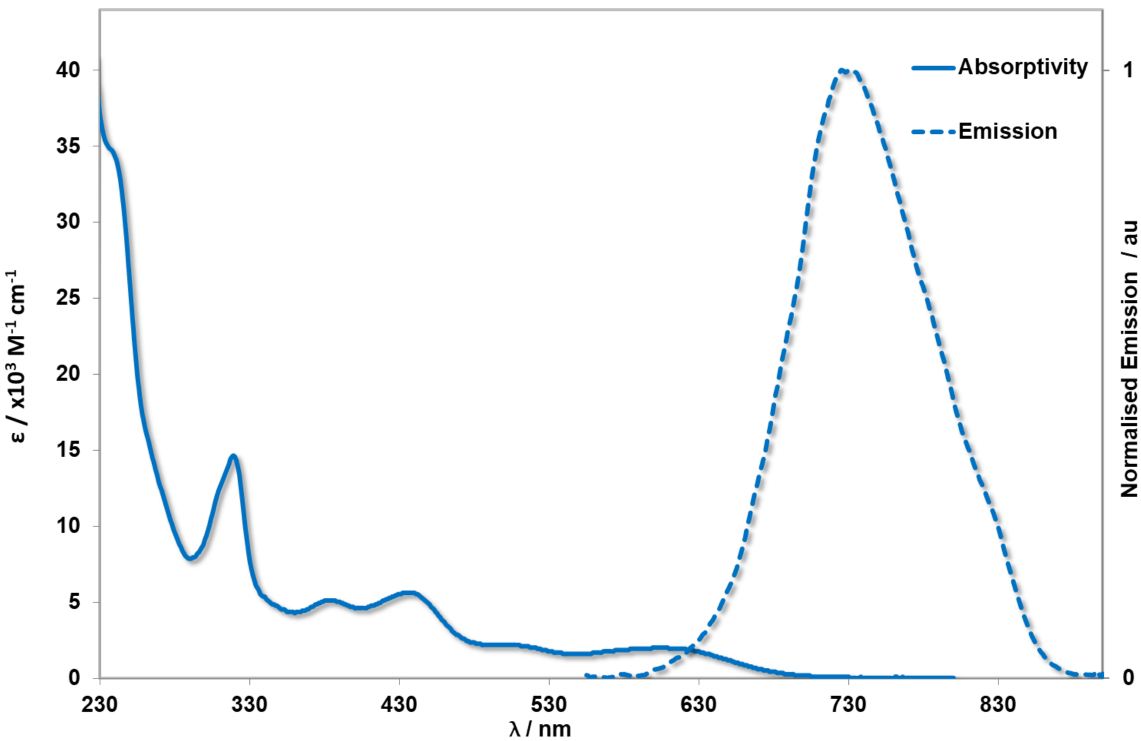

Figure **5.** The absorptivity (solid line) and photoluminescence spectra (dotted line) of **1** in CH_2Cl_2 at 298 K (c = 10^{-5} M).

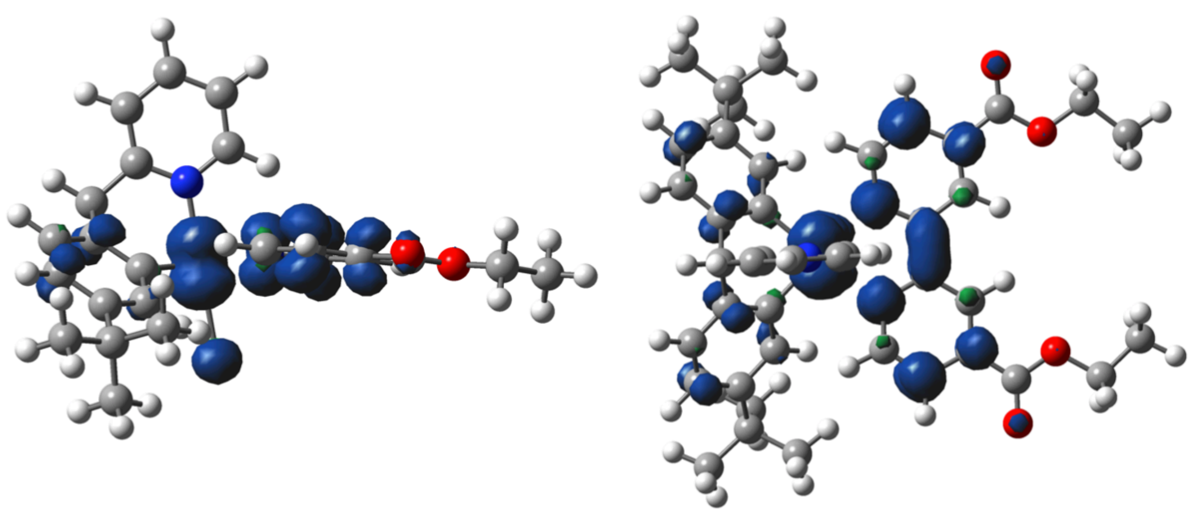

Figure **6.** DFT computed spin density difference plots for the lowest triplet state of **1**. Both side and top views are shown and they have been drawn with a contour threshold of 3 × 10^{-3} au.

Table **2.** Photophysical properties of complex **1**.

Complex	λ_{abs} / nm (ε / $M^{-1}cm^{-1}$)^a	$\lambda_{em}{}^b$ / nm	$\Phi_{PL}{}^{b,c}$ / %	$\tau_e{}^d$ / ns
1	237 (34819), 319 (14647), 384 (5105), 434 (5607), 504 (2176), 597 (1925)	731	0.5	36 (73 %) 78 (19 %) 392 (8 %)

^{a} Recorded in aerated CH_2Cl_2 at 298 K; ^{b} Recorded at 298 K in deaerated CH_2Cl_2 solution (λ_{exc} = 420 nm); ^{c} $[Ru(bpy)_3](PF_6)_2$ in MeCN as the reference (Φ_{PL} = 1.8% in aerated MeCN at 298 K)[52]; ^{d} λ_{exc} = 378 nm.

Dye-sensitized solar cells (DSSCs)

Sandwich-type solar cells were assembled using **1-**sensitised nanocrystalline TiO_2 as the working electrodes, platinized conducting glass as the counter electrode and iodide/triiodide in acetonitrile as electrolyte. The photovoltaic performances of solar cells based **1** and **N719**, as benchmark sensitizer, are summarized in Table **3**. Figure **7** shows the current–voltage characteristics of the dyes under AM 1.5 simulated sunlight (100 mW cm^{-2}) and in the dark.

Table **3**. Photovoltaic performance of **1**.

DYE	$J_{SC}{}^a$ **/ mA cm^{-2}**	$V_{OC}{}^a$ **/ V**	**FF^a**	η^a **/ %**
1	0.995	0.67	0.74	0.49
N719	8.84	0.81	0.61	4.4

$^a J_{sc}$ is the short-circuit current density at the V = 0 intercept, V_{oc} is the open-circuit voltage at the J = 0 intercept, FF is the device fill factor, η is the power conversion efficiency.

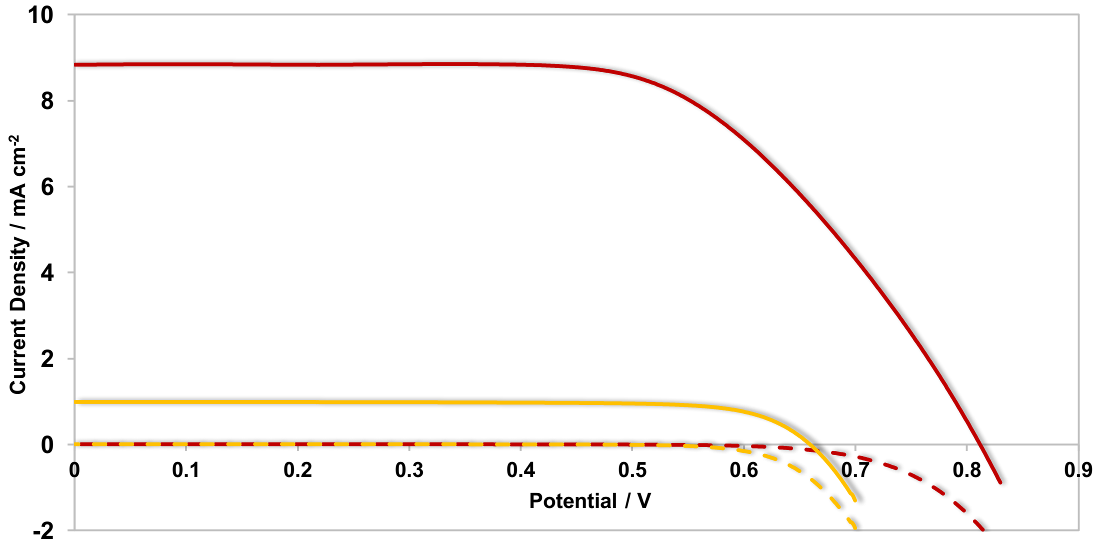

Figure **7**. Current-voltage curves for DSSCs constructed using **1** (orange) and **N719** (red) in the dark (dashed line) and under simulated sunlight (solid line, AM1.5, 100 mW cm^{-2}).

The photovoltaic efficiency (η = 0.49%) obtained with **1** is low, but comparable with results for iridium sensitizers reported elsewhere.[10,9,8,7,5] Both charge injection from the excited dye into TiO_2 and regeneration by the electrolyte are thermodynamically favourable. The fill factor for the N719 device (0.61) was slightly lower than that typically obtained in optimized devices (0.70-0.75) and the shape of the current-voltage curve is consistent with high series resistance. Procedures used in optimized N719 devices, such as mixed solvents or additives such as chenodeoxycholic acid in the electrolyte or dye bath are likely to improve the performance of the N719 devices, however the conditions chosen were optimal for compound **1**. We therefore attribute the reason for the low efficiency for **1** compared to the benchmark Ru dye to be the weak absorption in the visible region, compared to ruthenium-based photosensitizers such as N719. The absorption spectrum of the TiO_2 electrode after immersion in the dye solution is provided in Figure **S13** and the spectral response of the DSSC is given in Figure **S14**. The low incident photon-to current conversion efficiency (IPCE < 2%) is consistent with the poor light-harvesting at $\lambda > 500$ nm. While these dyes absorb broadly across the visible spectrum, the low ε ($\varepsilon \sim 2\ 000\ M^{-1}\ cm^{-1}$) compared to ruthenium dyes ($\varepsilon > 10\ 000\ M^{-1}\ cm^{-1}$) is a limitation to their solar cell performance.

Conclusions

In conclusion, a new panchromatically absorbing, NIR luminescent iridium(III) complexes bearing a tripodal tris(six-membered) chelate ligand has been obtained and comprehensively characterized, including by single crystal X-ray diffraction. The absorption spectrum tails off at 700 nm, much further than most neutral iridium complexes while the emission is significantly shifted into the NIR, with a maximum of 731 nm. DSSCs using **1** as the dye achieved only modest efficiency of 0.49%, comparable to other Ir(III) dyes. This was attributed to the modest absorption coefficient, which leads to weak light harvesting in the visible region and low short-circuit current.

Appendix A. Supplementary data

CCDC 1583853 contains the supplementary crystallographic data for **1**. These data can be obtained free of charge via http://www.ccdc.cam.ac.uk/conts/retrieving.html, or from the Cambridge Crystallographic Data Centre, 12 Union Road, Cambridge CB2 1EZ, UK; fax: (+44) 1223-336-033; or e-mail: deposit@ccdc.cam.ac.uk. NMR and MS spectra for **1**, Supplementary crystallographic data, supplementary electrochemical and photophysical data. Description of the DFT/TD-DFT protocol. Experimental details for the DSSC assembly and testing. Plots of the absorption spectra of **1**-sensitized TiO_2 and IPCE spectrum of the DSSC.

Acknowledgements

C.H. acknowledges the *Région Bretagne*, France for funding. EZ-C acknowledges the University of St Andrews and EPSRC (EP/M02105X/1) for financial support. We thank Umicore AG for the gift of materials. We thank the EPSRC UK National Mass Spectrometry Facility at Swansea University for analytical services. This research used computational resources of 1) the GENCI-CINES/IDRIS, 2) the CCIPL (C*entre de Calcul Intensif des Pays de Loire*), 3) a local Troy cluster. EAG and HVF thank the ERC for a Starting Grant (p-TYPE, 715354).

References

1. Henwood, A.F., Zysman-Colman, E.: A Comprehensive Review of Luminescent Iridium Complexes Used in Light-Emitting Electrochemical Cells (LEECs). In: Iridium(III) in Optoelectronic and Photonics Applications. pp. 275-357. John Wiley & Sons, Ltd, (2017)
2. Longhi, E., De Cola, L.: Iridium(III) Complexes for OLED Application. In: Iridium(III) in Optoelectronic and Photonics Applications. pp. 205-274. John Wiley & Sons, Ltd, (2017)
3. Mayo, E.I., Kilsa, K., Tirrell, T., Djurovich, P.I., Tamayo, A., Thompson, M.E., Lewis, N.S., Gray, H.B.: Cyclometalated iridium(iii)-sensitized titanium dioxide solar cells. Photochem. Photobiol. Sci **5**(10), 871-873 (2006).
4. Yuan, Y.-J., Zhang, J.-Y., Yu, Z.-T., Feng, J.-Y., Luo, W.-J., Ye, J.-H., Zou, Z.-G.: Impact of Ligand Modification on Hydrogen Photogeneration and Light-Harvesting Applications Using Cyclometalated Iridium Complexes. Inorg. Chem. **51**, 4123-4133 (2012). doi:10.1021/ic202423y
5. Dragonetti, C., Valore, A., Colombo, A., Righetto, S., Trifiletti, V.: Simple novel cyclometallated iridium complexes for potential application in dye-sensitized solar cells. Inorg. Chim. Acta **388**(0), 163-167 (2012). doi:10.1016/j.ica.2012.03.028
6. Ning, Z., Zhang, Q., Wu, W., Tian, H.: Novel iridium complex with carboxyl pyridyl ligand for dye-sensitized solar cells: High fluorescence intensity, high electron injection efficiency? J. Organomet. Chem. **694**(17), 2705-2711 (2009). doi:10.1016/j.jorganchem.2009.02.016
7. Baranoff, E., Yum, J.-H., Graetzel, M., Nazeeruddin, M.K.: Cyclometallated iridium complexes for conversion of light into electricity and electricity into light. J. Organomet. Chem. **694**(17), 2661-2670 (2009). doi:10.1016/j.jorganchem.2009.02.033
8. Baranoff, E., Yum, J.-H., Jung, I., Vulcano, R., Grätzel, M., Nazeeruddin, M.K.: Cyclometallated Iridium Complexes as Sensitizers for Dye-Sensitized Solar Cells. Chem. Asian J. **5**(3), 496-499 (2010). doi:10.1002/asia.200900429
9. Sinopoli, A., Wood, C.J., Gibson, E.A., Elliott, P.I.P.: New cyclometalated iridium(III) dye chromophore complexes for n-type dye-sensitised solar cells. Inorg. Chim. Acta **457**, 81-89 (2017). doi:10.1016/j.ica.2016.12.003

10. Sinopoli, A., Wood, C.J., Gibson, E.A., Elliott, P.I.P.: Hybrid Cyclometalated Iridium Coumarin Complex as a Sensitiser of Both n- and p-Type DSSCs. Eur. J. Inorg. Chem. **2016**(18), 2887-2890 (2016). doi:10.1002/ejic.201600242
11. Wang, D., Wu, Y., Dong, H., Qin, Z., Zhao, D., Yu, Y., Zhou, G., Jiao, B., Wu, Z., Gao, M., Wang, G.: Iridium (III) complexes with 5,5-dimethyl-3-(pyridin-2-yl)cyclohex-2-enone ligands as sensitizer for dye-sensitized solar cells. Org. Electron. **14**(12), 3297-3305 (2013). doi:10.1016/j.orgel.2013.09.040
12. Shinpuku, Y., Inui, F., Nakai, M., Nakabayashi, Y.: Synthesis and characterization of novel cyclometalated iridium(III) complexes for nanocrystalline TiO2-based dye-sensitized solar cells. J. Photochem. Photobiol., A **222**(1), 203-209 (2011). doi:10.1016/j.jphotochem.2011.05.023
13. Gennari, M., Légalité, F., Zhang, L., Pellegrin, Y., Blart, E., Fortage, J., Brown, A.M., Deronzier, A., Collomb, M.-N., Boujtita, M., Jacquemin, D., Hammarström, L., Odobel, F.: Long-Lived Charge Separated State in NiO-Based p-Type Dye-Sensitized Solar Cells with Simple Cyclometalated Iridium Complexes. The Journal of Physical Chemistry Letters **5**(13), 2254-2258 (2014). doi:10.1021/jz5009714
14. Henwood, A.F., Hu, Y., Sajjad, M.T., Thalluri, G.K., Ghosh, S.S., Cordes, D.B., Slawin, A.M., Samuel, I.D., Robertson, N., Zysman-Colman, E.: Unprecedented Strong Panchromic Absorption from Proton-Switchable Iridium(III) Azoimidazolate Complexes. Chem. Eur. J. **21**(52), 19128-19135 (2015). doi:10.1002/chem.201503546
15. Hasan, K., Zysman-Colman, E.: Panchromic Cationic Iridium(III) Complexes. Inorg. Chem. **ASAP**, DOI: 10.1021/ic301998t (2012). doi:10.1021/ic301998t
16. Tamayo, A.B., Garon, S., Sajoto, T., Djurovich, P.I., Tsyba, I.M., Bau, R., Thompson, M.E.: Cationic Bis-cyclometalated Iridium(III) Diimine Complexes and Their Use in Efficient Blue, Green, and Red Electroluminescent Devices. Inorg. Chem. **44**(24), 8723-8732 (2005). doi:10.1021/ic050970t
17. Zhao, Q., Liu, S., Shi, M., Wang, C., Yu, M., Li, L., Li, F., Yi, T., Huang, C.: Series of New Cationic Iridium(III) Complexes with Tunable Emission Wavelength and Excited State Properties: Structures, Theoretical Calculations, and Photophysical and Electrochemical Properties. Inorg. Chem. **45**(16), 6152-6160 (2006). doi:doi:10.1021/ic052034j
18. Medina-Castillo, A.L., Fernandez-Sanchez, J.F., Klein, C., Nazeeruddin, M.K., Segura-Carretero, A., Fernandez-Gutierrez, A., Graetzel, M., Spichiger-Keller, U.E.: Engineering of efficient phosphorescent iridium cationic complex for developing oxygen-sensitive polymeric and nanostructured films. Analyst **132**(9), 929-936 (2007).
19. Aubert, V., Ordronneau, L., Escadeillas, M., Williams, J.A.G., Boucekkine, A., Coulaud, E., Dragonetti, C., Righetto, S., Roberto, D., Ugo, R., Valore, A., Singh, A., Zyss, J., Ledoux-Rak, I., Le Bozec, H., Guerchais, V.r.: Linear and Nonlinear Optical Properties of Cationic Bipyridyl Iridium(III) Complexes: Tunable and Photoswitchable? Inorg. Chem. **50**(11), 5027-5038 (2011). doi:10.1021/ic2002892
20. Kammer, S., Starke, I., Pietrucha, A., Kelling, A., Mickler, W., Schilde, U., Dosche, C., Kleinpeter, E., Holdt, H.-J.: 1,12-Diazaperylene and 2,11-dialkylated-1,12-diazaperylene iridium(iii) complexes [Ir(C^N)2(N^N)]PF6: new supramolecular assemblies. Dalton Trans. **41**(34), 10219-10227 (2012).
21. Hierlinger, C., Roisnel, T., Cordes, D.B., Slawin, A.M.Z., Jacquemin, D., Guerchais, V., Zysman-Colman, E.: An Unprecedented Family of Luminescent Iridium(III) Complexes

Bearing a Six-Membered Chelated Tridentate C^N^C Ligand. Inorg Chem **56**(9), 5182-5188 (2017). doi:10.1021/acs.inorgchem.7b00328
22. He, W.Y., Fontmorin, J.M., Hapiot, P., Soutrel, I., Floner, D., Fourcade, F., Amrane, A., Geneste, F.: A new bipyridyl cobalt complex for reductive dechlorination of pesticides. Electrochim. Acta **207**, 313-320 (2016). doi:10.1016/j.electacta.2016.04.170
23. Koga, Y., Kamo, M., Yamada, Y., Matsumoto, T., Matsubara, K.: Synthesis, Structures, and Unique Luminescent Properties of Tridentate C∧C∧N Cyclometalated Complexes of Iridium. Eur. J. Inorg. Chem. **2011**(18), 2869-2878 (2011). doi:10.1002/ejic.201100055
24. Obara, S., Itabashi, M., Okuda, F., Tamaki, S., Tanabe, Y., Ishii, Y., Nozaki, K., Haga, M.-a.: Highly Phosphorescent Iridium Complexes Containing Both Tridentate Bis(benzimidazolyl)-benzene or -pyridine and Bidentate Phenylpyridine: Synthesis, Photophysical Properties, and Theoretical Study of Ir-Bis(benzimidazolyl)benzene Complex. Inorg. Chem. **45**(22), 8907-8921 (2006). doi:doi:10.1021/ic060796o
25. Brulatti, P., Gildea, R.J., Howard, J.A.K., Fattori, V., Cocchi, M., Williams, J.A.G.: Luminescent Iridium(III) Complexes with N∧C∧N-Coordinated Terdentate Ligands: Dual Tuning of the Emission Energy and Application to Organic Light-Emitting Devices. Inorg. Chem. **51**(6), 3813-3826 (2012). doi:10.1021/ic202756w
26. Ashizawa, M., Yang, L., Kobayashi, K., Sato, H., Yamagishi, A., Okuda, F., Harada, T., Kuroda, R., Haga, M.A.: Syntheses and photophysical properties of optical-active blue-phosphorescent iridium complexes bearing asymmetric tridentate ligands. Dalton Trans(10), 1700-1702 (2009). doi:10.1039/b820821m
27. Daniels, R.E., Culham, S., Hunter, M., Durrant, M.C., Probert, M.R., Clegg, W., Williams, J.A., Kozhevnikov, V.N.: When two are better than one: bright phosphorescence from non-stereogenic dinuclear iridium(III) complexes. Dalton Trans **45**(16), 6949-6962 (2016). doi:10.1039/c6dt00881j
28. Yoshikawa, N., Sakamoto, J., Kanehisa, N., Kai, Y., Matsumura-Inoue, T., Takashima, H., Tsukahara, K.: (4,4′-Dimethyl-2,2′-bipyridine)chloro-(2,2′:6′,2″-terpyridine)-iridium(III) hexafluorophosphate. Acta Cryst. E **59**(10), m830-m832 (2003). doi:10.1107/s1600536803019081
29. Hanss, D., Freys, J.C., Bernardinelli, G., Wenger, O.S.: Cyclometalated Iridium(III) Complexes as Photosensitizers for Long-Range Electron Transfer: Occurrence of a Coulomb Barrier. Eur. J. Inorg. Chem. **2009**(32), 4850-4859 (2009). doi:10.1002/ejic.200900673
30. Henwood, A.F., Pal, A.K., Cordes, D.B., Slawin, A.M.Z., Rees, T.W., Momblona, C., Babaei, A., Pertegas, A., Orti, E., Bolink, H.J., Baranoff, E., Zysman-Colman, E.: Blue-emitting cationic iridium(iii) complexes featuring pyridylpyrimidine ligands and their use in sky-blue electroluminescent devices. J. Mater. Chem. C **5**(37), 9638-9650 (2017). doi:10.1039/C7TC03110F
31. Costa, R.D., Ortì, E., Bolink, H.J., Graber, S., Schaffner, S., Neuburger, M., Housecroft, C.E., Constable, E.C.: Archetype Cationic Iridium Complexes and Their Use in Solid-State Light-Emitting Electrochemical Cells. Adv. Funct. Mater. **19**(21), 3456-3463 (2009). doi:10.1002/adfm.200900911
32. Ladouceur, S., Fortin, D., Zysman-Colman, E.: The role of substitution on the photophysical propertiesof 5,5'-diaryl-2,2'-bipyridine (bpy*) in [Ir(ppy)2(bpy*)]PF6 complexes: A

combined experimental and theoretical study. Inorg. Chem. **49**(12), 5625-5641 (2010). doi:10.1021/ic100521t/
33. Liu, S.-J., Zhao, Q., Fan, Q.-L., Huang, W.: A Series of Red-Light-Emitting Ionic Iridium Complexes: Structures, Excited State Properties, and Application in Electroluminescent Devices. Eur. J. Inorg. Chem. **2008**(13), 2177-2185 (2008). doi:10.1002/ejic.200701184
34. Cardona, C.M., Li, W., Kaifer, A.E., Stockdale, D., Bazan, G.C.: Electrochemical Considerations for Determining Absolute Frontier Orbital Energy Levels of Conjugated Polymers for Solar Cell Applications. Adv. Mater. **23**(20), 2367-2371 (2011). doi:10.1002/adma.201004554
35. Chirdon, D.N., McCusker, C.E., Castellano, F.N., Bernhard, S.: Tracking of Tuning Effects in Bis-Cyclometalated Iridium Complexes: A Combined Time Resolved Infrared Spectroscopy, Electrochemical, and Computational Study. Inorg. Chem. **52**(15), 8795-8804 (2013). doi:10.1021/ic401009q
36. Pavlishchuk, V.V., Addison, A.W.: Conversion constants for redox potentials measured versus different reference electrodes in acetonitrile solutions at 25°C. Inorg. Chim. Acta **298**(1), 97-102 (2000). doi:10.1016/s0020-1693(99)00407-7
37. Connelly, N.G., Geiger, W.E.: Chemical Redox Agents for Organometallic Chemistry. Chem. Rev. **96**, 877-910 (1996).
38. Zhao, Q., Yu, M., Shi, L., Liu, S., Li, C., Shi, M., Zhou, Z., Huang, C., Li, F.: Cationic Iridium(III) Complexes with Tunable Emission Color as Phosphorescent Dyes for Live Cell Imaging. Organometallics **29**(5), 1085-1091 (2010). doi:10.1021/om900691r
39. Ertl, C.D., Momblona, C., Pertegás, A., Junquera-Hernández, J.M., La-Placa, M.-G., Prescimone, A., Ortí, E., Housecroft, C.E., Constable, E.C., Bolink, H.J.: Highly Stable Red-Light-Emitting Electrochemical Cells. J. Am. Chem. Soc. **139**(8), 3237-3248 (2017). doi:10.1021/jacs.6b13311
40. Pal, A.K., Cordes, D.B., Slawin, A.M.Z., Momblona, C., Pertegas, A., Orti, E., Bolink, H.J., Zysman-Colman, E.: Simple design to achieve red-to-near-infrared emissive cationic Ir(iii) emitters and their use in light emitting electrochemical cells. RSC Advances **7**(51), 31833-31837 (2017). doi:10.1039/C7RA06347D
41. Kesarkar, S., Mróz, W., Penconi, M., Pasini, M., Destri, S., Cazzaniga, M., Ceresoli, D., Mussini, P.R., Baldoli, C., Giovanella, U., Bossi, A.: Near-IR Emitting Iridium(III) Complexes with Heteroaromatic β-Diketonate Ancillary Ligands for Efficient Solution-Processed OLEDs: Structure–Property Correlations. Angew. Chem. Int. Ed. **55**(8), 2714-2718 (2016). doi:10.1002/anie.201509798
42. Xin, L., Xue, J., Lei, G., Qiao, J.: Efficient near-infrared-emitting cationic iridium complexes based on highly conjugated cyclometalated benzo[g]phthalazine derivatives. RSC Adv. **5**(53), 42354-42361 (2015). doi:10.1039/c5ra04511h
43. Zhang, G., Zhang, H., Gao, Y., Tao, R., Xin, L., Yi, J., Li, F., Liu, W., Qiao, J.: Near-Infrared-Emitting Iridium(III) Complexes as Phosphorescent Dyes for Live Cell Imaging. Organometallics **33**(1), 61-68 (2013). doi:10.1021/om400676h
44. Bixon, M., Jortner, J., Cortes, J., Heitele, H., Michel-Beyerle, M.E.: Energy Gap Law for Nonradiative and Radiative Charge Transfer in Isolated and in Solvated Supermolecules. J. Phys. Chem. **98**(30), 7289-7299 (1994). doi:10.1021/j100081a010
45. Caspar, J.V., Meyer, T.J.: Application of the energy gap law to nonradiative, excited-state decay. J. Phys. Chem. **87**(6), 952-957 (1983). doi:10.1021/j100229a010

46. Tao, R., Qiao, J., Zhang, G., Duan, L., Wang, L., Qiu, Y.: Efficient Near-Infrared-Emitting Cationic Iridium Complexes as Dopants for OLEDs with Small Efficiency Roll-off. J. Phys. Chem. C **116**(21), 11658-11664 (2012). doi:10.1021/jp301740c
47. Hasan, K., Bansal, A.K., Samuel, I.D.W., Roldán-Carmona, C., Bolink, H.J., Zysman-Colman, E.: Tuning the Emission of Cationic Iridium (III) Complexes Towards the Red Through Methoxy Substitution of the Cyclometalating Ligand. Scientific Reports **5**, 12325 (2015). doi:10.1038/srep12325

http://www.nature.com/articles/srep12325 - supplementary-information
48. Wang, L., Yin, H., Cui, P., Hetu, M., Wang, C., Monro, S., Schaller, R.D., Cameron, C.G., Liu, B., Kilina, S., McFarland, S.A., Sun, W.: Near-infrared-emitting heteroleptic cationic iridium complexes derived from 2,3-diphenylbenzo[g]quinoxaline as in vitro theranostic photodynamic therapy agents. Dalton Trans. **46**(25), 8091-8103 (2017). doi:10.1039/C7DT00913E
49. Xin, L., Xue, J., Lei, G., Qiao, J.: Efficient near-infrared-emitting cationic iridium complexes based on highly conjugated cyclometalated benzo[g]phthalazine derivatives. RSC Advances **5**(53), 42354-42361 (2015). doi:10.1039/C5RA04511H
50. Cao, X., Miao, J., Zhu, M., Zhong, C., Yang, C., Wu, H., Qin, J., Cao, Y.: Near-Infrared Polymer Light-Emitting Diodes with High Efficiency and Low Efficiency Roll-off by Using Solution-Processed Iridium(III) Phosphors. Chem. Mater. **27**(1), 96-104 (2015). doi:10.1021/cm503361j
51. Tao, R., Qiao, J., Zhang, G., Duan, L., Chen, C., Wang, L., Qiu, Y.: High-efficiency near-infrared organic light-emitting devices based on an iridium complex with negligible efficiency roll-off. J. Mater. Chem. C **1**(39), 6446-6454 (2013). doi:10.1039/C3TC30866A
52. Suzuki, K., Kobayashi, A., Kaneko, S., Takehira, K., Yoshihara, T., Ishida, H., Shiina, Y., Oishi, S., Tobita, S.: Reevaluation of absolute luminescence quantum yields of standard solutions using a spectrometer with an integrating sphere and a back-thinned CCD detector. Phys Chem Chem Phys **11**(42), 9850-9860 (2009). doi:10.1039/b912178a

TOC

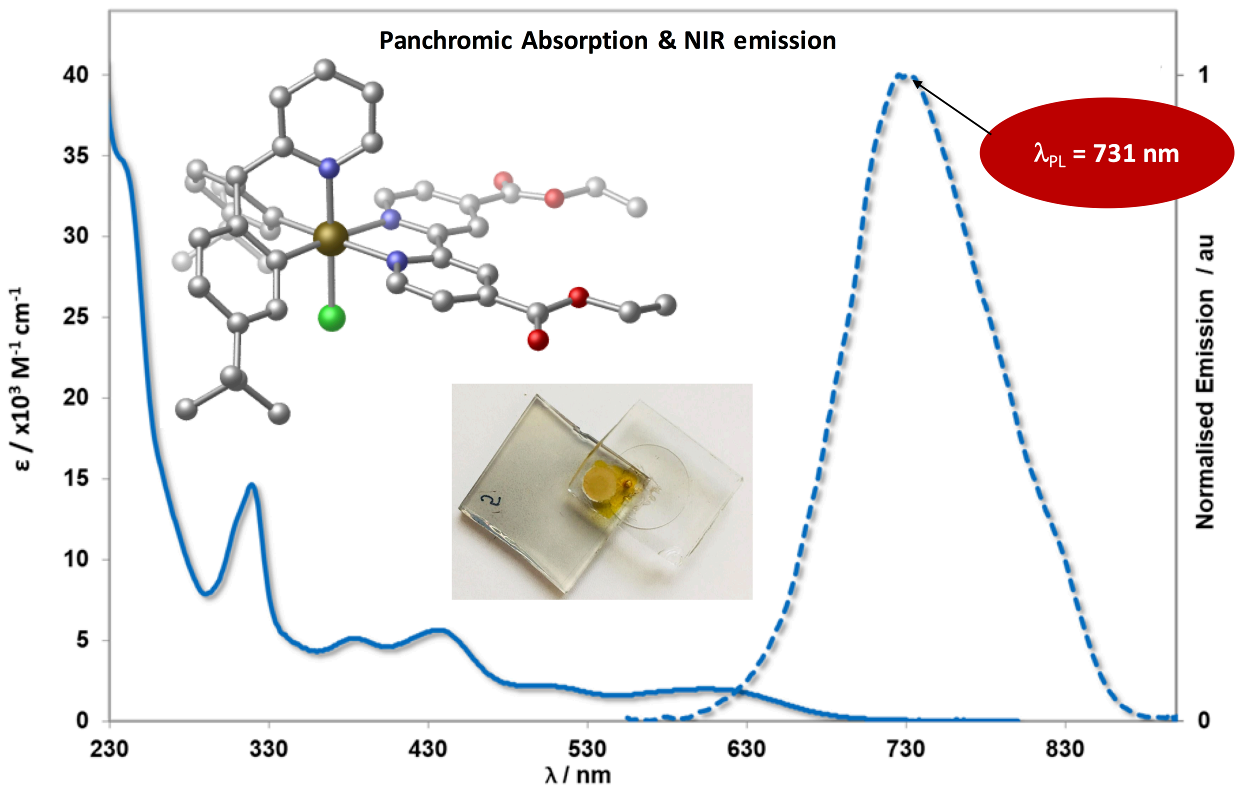
Panchromic Absorption & NIR emission
λPL = 731 nm
ε / x10³ M⁻¹ cm⁻¹
Normalised Emission / au
λ / nm
40
35
30
25
20
15
10
5
0
1
0
230
330
430
530
630
730
830